spin glass. In the range of high concentrations of magnetic atoms, not shown in the figure, the high-order cumulants decrease rapidly with increase of the concentration. In this range, the distribution of molecular fields is nearly normal in agreement with formulas (28) and (33). But for the spin-glass phase near T_g, such concentrations are unattainable because of the transition to the ferromagnetic state. For example, near the phase boundary $T_g = 4.4 \cdot 10^{-2} J_0$ the coefficient of excess is $\varkappa_4'/\varkappa_2'^2 = 5.9$, whereas for the normal distribution it is zero. This means that for adequate description of the spin-glass phase, it is insufficient to consider only two equations of the system (8) (with $\varkappa_k = 0$ for $k \geqslant 3$); it is necessary to study the complete system or the integral equation (6).

In conclusion, the author expresses his deep gratitude to S. L. Ginzburg for formulation of the problem and for numerous discussions and to S. V. Sardaryan for his friendly interest in the research and for a number of valuable comments.

APPENDIX

Derivation of formula (A.1)

From the definition (22) of the kernel $N^{(i)}(\rho, y)$ we have

$$L_k - \mathrm{N}^{(i)} L_k = (1 - \nu_i \nu_k^{-1}) L_k + (L_i, L_k)_\varphi \varphi M_i.$$

We perform an inverse linear transformation:

$$L_k = (1 - \nu_i \nu_k^{-1})(L_k + \mathrm{R}^{(i)} L_k) + (L_i, L_k)_\varphi (\varphi M_i + \mathrm{R}^{(i)} \varphi M_i). \quad (A.2)$$

For $i = k$, formula (A.2) takes the form

$$L_i = \varphi M_i + \mathrm{R}^{(i)} \varphi M_i. \quad (A.3)$$

On substituting (A.3) in (A.2), we get for $i \neq k$ formula (A.1); see § 5.

[1] I. Ya. Korenblit and E. F. Shender, Usp. Fiz. Nauk **126**, 233 (1978) [Sov. Phys. Usp. **21**, 832 (1978)]; Zh. Eksp. Teor. Fiz. **62**, 1949 (1972) [Sov. Phys. JETP **35**, 1017 (1972)].
[2] M. W. Klein and R. Brout, Phys. Rev. **132**, 2412 (1963).
[3] M. W. Klein, Phys. Rev. **173**, 552 (1968); **B14**, 5008 (1976).
[4] S. L. Ginzburg, Zh. Eksp. Teor. Fiz. **74**, 236 (1978) [Sov. Phys. JETP **47**, 121 (1978)].
[5] M. M. Vaĭnberg and V. A. Trenogin, Teoriya vetvleniya reshenii nelineĭnykh uravnenii (Theory of Branching of Solutions of Nonlinear Equations), Nauka, 1969, p. 226 (transl., Noordhoff Intl. Pub., Leyden, 1974; German transl., Akademie-Verlag, Berlin, 1973).
[6] G. Marchal, Ph. Mangin, and Chr. Janot, Solid State Commun. **18**, 739 (1976).
[7] B. H. Verbeek, C. Van Dijk, C. J. Nieuwenhuys, and J. A. Mydosh, J. Phys. (Paris) **39**, Suppl., C6-918 (1978).
[8] D. E. Murnick, A. T. Fiory, and W. J. Kossler, Phys. Rev. Lett. **36**, 100 (1976).
[9] L. R. Walker and R. E. Walstedt, Phys. Rev. Lett. **38**, 514 (1977).
[10] C. Domb, Adv. Phys. **9**, 149 (1960).
[11] D. Sherrington and S. Kirkpatrick, Phys. Rev. Lett. **35**, 1792 (1975).
[12] S. Kirkpatrick and D. Sherrington, Phys. Rev. **B17**, 4384 (1978).
[13] N. G. Chebotarev, Sobranie Sochinenii (Collected Works), Vol. 3, Izd. Akad. Nauk SSSR, 1950, p. 47.
[14] S. F. Edwards and P. W. Anderson, J. Phys. F **5**, 965 (1975).
[15] A. P. Murani, J. Phys. (Paris) **39**, Suppl., C6-1517 (1978).

Translated by W. F. Brown, Jr.

Magnetic linear birefringence of light and dichroism in the region of the absorption band of the rare-earth ion in europium iron garnet

G. S. Krinchik, V. D. Gorbunova, V. S. Gushchin, and A. A. Kostyarin

Moscow State University
(Submitted 1 August 1979)
Zh. Eksp. Teor. Fiz. **78**, 869–879 (Feburary 1980)

Results are reported of a spectroscopic investigation, by a polarization magneto-optical procedure, of the optical transition $^7F_0 \rightarrow {}^7F_6$ of the Eu^{3+} ion in the structure of europium iron garnet. It is shown that in the employed Voigt geometry the magnetic linear birefringence and the dichroism reach values 10^{-3}, and have a strong dependence on the wavelength and a strong anisotropy. For a sample cut in the (110) plane, comparison shows that the spectra for the cases I||[$\bar{1}$10], e||[001] and I||[001], e||[$\bar{1}$10] differ noticeably. The known formulas for δn and δk (the contribution due to I to n and k), which describe well the magnetic birefrigence and the dichroism of cubic crystals far from the absorption line, are invariant to interchange of the directions of I and e. A model-based theory is proposed to explain the observed independence of the spectra as being due to the low local symmetry of the surrounding of magnetically active ions in the crystal.

PACS numbers: 78.20.Ls, 78.50.Ge

1. INTRODUCTION

Investigation of magnetic birefringence (MB) of light by magnetically ordered crystals is attracting much interest of late. A large value of the magnetic linear birefringence was first discovered by Dillon[1] in an yttrium iron garnet crystal, and used to observe the domain structure. It was shown in Ref. 2 that the mag-

 0038-5646/80/020435-07$02.40

netic linear dichroism, and consequently also the magnetic birefringence in the region of the transmission band $^7F_0 \rightarrow {}^7F_4$ of the rare-earth (RE) ion Eu^{3+} reaches large values, of the order of 4×10^{-3}. Detailed investigations of the magnetic linear birefringence in various iron garnets (IG) in the transparency region are reported in Ref. 3, where attention was called for the first time to the unexpected circumstance that in magnetic crystals the magnetic circular and linear birefringence of light are of the same order of magnitude. As a rule, measurements of MB were made at fixed laser wavelengths; this decreased the amount of information obtained from the experiments and, in particular, did not make it possible to use magnetic birefringence and dichroism to investigate the electronic structure of the energy spectrum of rare-iron ions in the structure of the IG. The solution of the last problem allows us to attack the more complicated and still unsolved problem of determining the spin Hamiltonian of RE ions in magnetically order IG crystals. The difficulty is that the low-symmetry crystal-field potential that acts on the RE ions of a paramagnetic crystal with garnet structure, and determines the splitting of the energy level with a given quantum number J, contains a large number of independent parameters, the numerical values of which cannot be calculated theoretically and must be obtained by experiment. The presence of exchange interaction in the ferrimagnetic IG crystal makes makes it necessary to determine the anisotropic G tensor of the exchange field.[4] In addition, at an arbitrary direction of the magnetizing field, the IG lattice contains 6 nonequivalent dodecahedral positions D_{2h} for the RE ions, and this complicates the problem even more. Up to now a more or less reliable determination of the spin Hamiltonian of a RE ion in an IG was effected only for the levels $^2F_{7/2}$ and $^2F_{5/2}$ of the Yb^{3+} ion with small value of J.[5] Attempts to determine the spin-Hamiltonian parameters for the RE ions Ho^{3+}, Er^{3+}, Eu^{3+}, Tb^{3+}, Nd^{3+}, Dy^{3+}, and others, with large values of J, from the optical-absorption, luminescence, and Raman spectra were also made in Ref. 6. However, greatest attention was paid there to paramagnetic crystals. Even though the problem seems more complicated for magnetically ordered crystals, some additional possibilities are afforded here, due to the fact that at a given orientation of the magnetization vector of the crystal the optical spectra are polarized. In magnetic crystals, because of the coupling of the spin and orbital moments of the RE ion, we are dealing not simply with optics but with magneto-optics or, in other words, with crystal optics governed governed by an external magnetic field.[7] By establishing experimentally the state of polarization of the fine-structure components of the absorption lines of the RE ions, it is possible to identify these absorption lines with definite optical transitions and determine, using several reliably identified energy levels, all the required parameters of the spin Hamiltonian.

We present here the results of experimental low-temperature investigations of the frequency dependence of the magnetic linear birefringence and dichroism in the Eu^{3+} ions in $Eu_3Fe_5O_{12}$ in the optical transition $^7F_0 \rightarrow {}^7F_6$ (4600–5200 cm^{-1}). We present also the dispersion curves of the absorption coefficient k and of the refractive index n for the given region of the spectrum, and establish the energy positions and the polarization characteristics of the individual fine-structure components of the given transition. It becomes possible thus to study the features of the crystal optics of magnetically ordered crystals in the region of the absorption band of magnetoactive ions, and also to obtain polarization characteristics of the spectra. This yields, when the selection rules are taken into account, reliable experimental material for the identification of the optical transitions.

2. MEASUREMENT PROCEDURE

The developed magneto-optical installation permits low-temperature measurements of a number of optical effects in transmitted light, namely, absorption of linearly and circularly polarized light in the presence of a magnetic field, the Faraday effect, and magnetic linear and circular dichroism. The spectra were automatically accorded with an EPP-09 automatic plotter, whose chart-drive shaft was cord-coupled to the rotary unit of the prisms of the DMR-4 monochromator. When the absorption spectra of the polarized light were registered the radiation intensity was modulated by a mechanical chopper—a flat screen secured to the moving rod of the GMK-1 mechanical-vibration generator. The motion of the recorder chart drive was synchronized with the sweep of the radiation spectrum; the radiation receiver was a PbS photoresistor. In the working energy band of the optical quanta 4600 – 5200 cm^{-1}, the magneto-optical spectra were recorded at monochromatic slit widths 0.03–0.1 mm, corresponding to a resolution 3–12 cm^{-1}.

The measurements were performed on single crystal plates of europium iron garnet 100 μm thick, cut in the three principal crystallographic planes (110), (100), and (111). In the investigations we used a metallic optical cryostat with a thin stub (~10 mm thick), which was inserted in the gap of an FL-1 electromagnetic capable of producing fields up to 22 kOe. The temperature of the sample mounted on the cooling copper holder was 82 K when the cryostat was filled with nitrogen. For measurements at various directions of the external magnetic field relative to the crystallographic axes, we used a manipulator that made it possible to rotate the sample in the cryostat without breaking the vacuum and to compare the spectra obtained for the same setting of the system. When the manipulator was used and the cryostat was filled with nitrogen, the sample temperature was 110° K. A comparison of the absorption spectra has shown that they vary little with temperature in the interval 110–82 °K.

3. EXPERIMENTAL RESULTS

Figure 1 shows the dispersion plots of the absorption coefficient k ($\tilde{n} = n - ik$), calculated from the experimental transmission spectra in the region of the $^7F_0 \rightarrow {}^7F_6$ absorption band for a plate cut in the (110) plane; the solid curve corresponds to the case $\mathbf{k} \| [110]$, $\mathbf{I} \| [001]$, $\mathbf{e} \| [\bar{1}10]$, and the dashed to the case $\mathbf{k} \| [110]$, $\mathbf{I} \| [001]$,

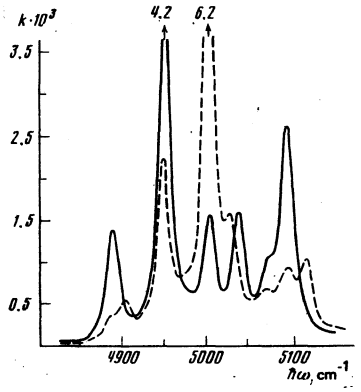

FIG. 1. Absorption spectra of europium iron garnet: solid line—for $\mathbf{k}\|[110]$, $\mathbf{I}\|[001]$, $\mathbf{e}\|[\bar{1}10]$; dashed—for $\mathbf{k}\|[110]$, $\mathbf{I}\|[001]$, $\mathbf{e}\|[001]$.

$\mathbf{e}\|[001]$ (σ and π components, respectively). At room temperature one broad absorption peak is observed from the π component, and two symmetrical absorption peaks for the σ component.[8] As seen from Fig. 1, when the temperature is lowered the general contour of the absorption curves of the σ and π components is preserved, but the band acquires a fine structure in which the individual components of the absorption are well resolved. The anisotropy of the absorption of the linearly polarized light manifests itself in the fact that the intensity of some of the peaks changes significantly when the electric vector of the light wave is rotated through 90° (magnetic linear dichroism Δk). The light transmission at $\hbar\omega = 4950$ cm^{-1} amounts to 7% for the σ component and to 25% for the π component, corresponding to $\Delta k = 2\times 10^{-3}$; at $\hbar\omega = 5000$ cm^{-1}, the light transmission is 37% for the σ component and 2% for the π component, corresponding to $\Delta k = 4.2\times 10^{-3}$. The frequencies of certain absorption peaks shift; peaks appear for the π component at $\hbar\omega = 4905$ and 5125 cm^{-1}. We note that it is these radical changes in the absorption spectrum when the plane of polarization of the light is rotated which provide the material that can be used, when the selection rules for the optical transitions are taken into account, to obtain the energy spectrum of the RE ion.

Using the Kramer-Kronig relations, a 15 VSM-5 computer was used to calculate the contribution made to the refractive index

$$n' = \frac{2}{\pi}\int \frac{k\omega\, d\omega}{\omega^2-\omega_0^2}$$

by the optical transition $^7F_0 \rightarrow {}^7F_6$ of the RE ion. The obtained plots of $n'(\hbar\omega)$ are shown in Fig. 2. It is seen from Fig. 2 that in the region of the absorption band the crystal exhibits considerable linear birefringence, reaching values 2×10^{-3}, for example, at $\hbar\omega = 4990$ cm^{-1} and $\hbar\omega = 5015$ cm^{-1}. The refractive indices n' for $\mathbf{e}\|[001]$ and $\mathbf{e}\|[\bar{1}10]$ depend on the light frequency in a complicated manner. In particular the intersection of these curves causes both positive and negative birefringence within the limits of the absorption band at different frequencies.

Figures 3 and 4 show plots of $k(\hbar\omega)$ and $n'(\hbar\omega)$ for the same sample in the case of magnetization along the $[\bar{1}11]$ axis. The solid curve is for the σ component

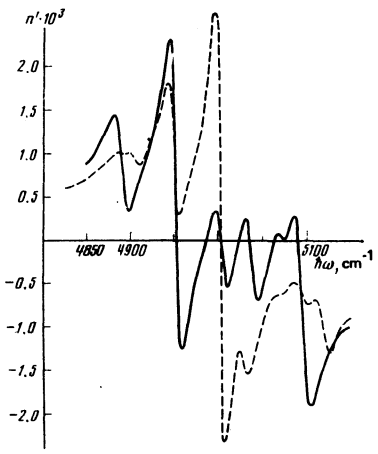

FIG. 2. Dependence of the contribution made to the refractive index n' ($\hbar\omega$) by the optical transition $^7F_0 \rightarrow {}^7F_6$ of the Eu^{3+} ion of europium iron garnet: solid line—for $\mathbf{k}\|[110]$, $\mathbf{I}\|[001]$, $\mathbf{e}\|[\bar{1}10]$; dashed—for $\mathbf{k}\|[110]$, $\mathbf{I}\|[001]$, $\mathbf{e}\|[001]$.

$\mathbf{I}\|[\bar{1}11]$, $\mathbf{e}\perp[\bar{1}11]$ and the dashed curve for the π component $\mathbf{I}\|[\bar{1}11]$, $\mathbf{e}\|[\bar{1}11]$. Here, too, an appreciable linear dichroism and birefringence are observed, especially in the energy regions 4950–4990 cm^{-1} and 5020–5040 cm^{-1}. The birefringence has opposite signs in these regions of the spectrum.

Figure 5 shows plots of $k(\hbar\omega)$ for a (110) plate at $\mathbf{I}\|[\bar{1}10]$, $\mathbf{e}\perp[\bar{1}10]$, i.e., $\mathbf{e}\|[001]$ (σ component, solid curve) and for $\mathbf{I}\|[\bar{1}10]$, $\mathbf{e}\|[110]$ (π component, dashed curve), as well as the σ component for the plate (100): $\mathbf{I}\|[\bar{1}10]$, $\mathbf{e}\perp[\bar{1}10]$, i.e., $\mathbf{e}\|[1\bar{1}0]$—dotted curve. In this case the solid and dotted curves correspond to magnetization of the sample along the [110] axis, but the electric vector of the light wave (perpendicular to the magnetization) is along different crystallographic directions. It is seen from Fig. 5 that the dispersion relations differ little from each other. Thus, in the case of magnetization along the [110] axis the crystal behaves like an optical uniaxial crystal. Figure 6 shows the plots of $n'(\hbar\omega)$ for this geometry, calculated from the Kramer-Kronig relations.

In the case of magnetization along the crystallographic axis [001], the dispersion curves $k(\hbar\omega)$ for the σ components (Fig. 7), in the case of measurements made on

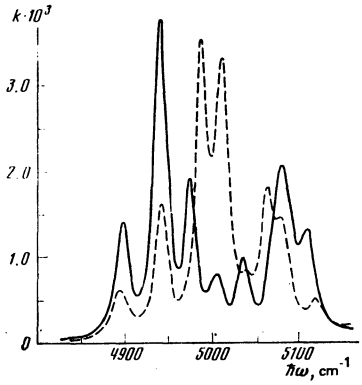

FIG. 3. Absorption spectra of europium iron garnet: solid line—for $\mathbf{k}\|[110]$, $\mathbf{I}\|[\bar{1}11]$, $\mathbf{e}\perp[\bar{1}11]$; dashed—for $\mathbf{k}\|[110]$, $\mathbf{I}\|[\bar{1}11]$, $\mathbf{e}\|[\bar{1}11]$.

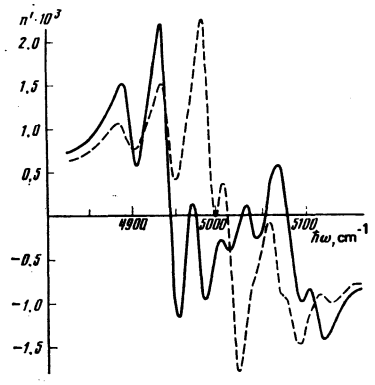

FIG. 4. Dependence of the contribution made to the refractive index n' ($\hbar\omega$) by the optical transition ${}^7F_0 \rightarrow {}^7F_6$ of the ion Eu^{3+} of europium iron garnet. Solid line—for $\mathbf{k} \| [110]$, $\mathbf{I} \| [\bar{1}11]$, $\mathbf{e} \perp [\bar{1}11]$; dashed—for $\mathbf{k} \| 110$, $\mathbf{I} \| [\bar{1}11]$, $\mathbf{e} \| [\bar{1}11]$.

a plate cut in the (110) plane, where $\mathbf{e} \| [\bar{1}10]$ (dashed curve), and a plate cut in the (100) plane, where $\mathbf{e} \| [010]$ (solid curve) coincide, thus confirming the requirement that a cubic crystal be optically homogeneous when magnetized along a fourfold axis. The corresponding π components, which are not shown in Fig. 7, also practically coincide.

To monitor the results obtained from magnetic birefringence (the $n'(\hbar\omega)$ curve calculated from the Kramer-Kronig relations) at different wavelengths, direct measurements of Δn were made using a Babinet-Soleil compensator. The measurements were made with the sample magnetized along the [001] axis, the light was linearly polarized at an angle 45° to this axis and propagated along the [110] axis [(110) plate]. Thus, we measured $\Delta n = n'_{[001]} - n'_{[\bar{1}10]}$. The following values were obtained: $\Delta n = 0.6 \cdot 10^{-3}$ at $\hbar\omega = 5080$ cm^{-1}, $\Delta n = 2.0 \cdot 10^{-3}$ at $\hbar\omega = 5020$ cm^{-1}, and $\Delta n = 1.9 \cdot 10^{-3}$ at $\hbar\omega = 4985$ cm^{-1}. Comparing the measured values of Δn with Fig. 2, which shows $n'_{[001]}$ and $n'_{[\bar{1}10]}$ calculated from the Kramer-Kronig relations, we can see that a calculation of the contribution to the refractive index, due to the optical transition ${}^7F_0 \rightarrow {}^7F_6$, provides a qualitatively correct picture of the behavior of $n'(\hbar\omega)$, although the more accurate numerical values can be expected in the

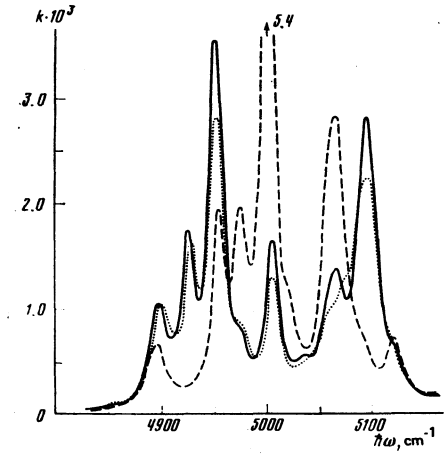

FIG. 5. Absorption spectra of europium iron garnet: solid line—for $\mathbf{k} \| [110]$, $\mathbf{I} \| [\bar{1}10]$, $\mathbf{e} \| [001]$; dashed—for $\mathbf{k} \| [110]$, $\mathbf{I} \| [\bar{1}10]$, $\mathbf{e} \| [\bar{1}10]$; dotted line—for $\mathbf{k} \| [001]$, $\mathbf{I} \| [\bar{1}10]$, $\mathbf{e} \| [1\bar{1}0]$.

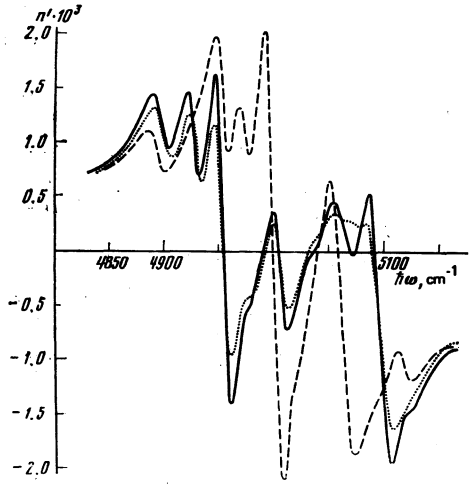

FIG. 6. Dependence of n' ($\hbar\omega$) of europium iron garnet: solid line—for $\mathbf{k} \| [110]$, $\mathbf{I} \| [\bar{1}10]$, $\mathbf{e} \| [001]$, dashed—for $\mathbf{k} \| [110]$, $\mathbf{I} \| [\bar{1}10]$, $\mathbf{e} \| [\bar{1}10]$; dotted line—for $\mathbf{k} \| [001]$, $\mathbf{I} \| [\bar{1}10]$, $\mathbf{e} \| [1\bar{1}0]$.

future. We note that the large values of the linear birefringence and dichroism, their anisotropy, and also their dependence on the orientation of the vector make it easy to "construct" in a crystal any specified combination of crystal-optics characteristics for the organization of one physical experiment or another.

The large values of the linear birefringence of RE iron garnet in the region of the absorbing bands uncovers also an interesting possibility of explaining the origin of the contribution of the RE sublattice to the magnetic linear birefringence of garnets in the region of their transparency.[3] It is quite possible that the contribution of the RE sublattice to the magnetic birefringence of the garnet at $\lambda_1 = 0.63$ μm and $\lambda_2 = 1.15$ μm is due mainly to the influence of the neighboring absorption bands of the RE ion, for example, in the case of $Eu_3Fe_5O_{12}$ to the influence of the nearest transitions ${}^7F_0 \rightarrow {}^7F_6$, ${}^7F_0 \rightarrow {}^7F_5$, ${}^7F_0 \rightarrow {}^7F_4$, ${}^7F_0 \rightarrow {}^5D$, and not to the influence of the transitions in the RE ions and Fe^{3+} ions, which are intense but lie in the far ultraviolet.

If we compare the solid curves of Fig. 1 ($\mathbf{k} \| [110]$, $\mathbf{I} \| [001]$, $\mathbf{e} \| [\bar{1}10]$) and of Fig. 5 ($\mathbf{k} \| [110]$, $\mathbf{I} \| [\bar{1}10]$,

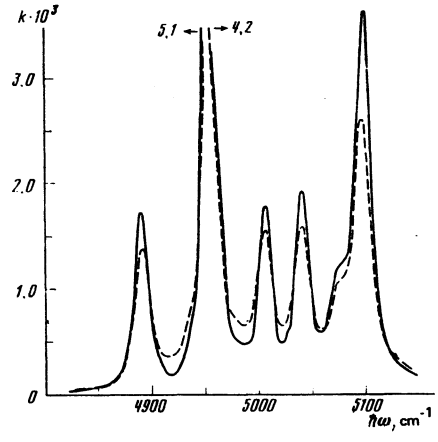

FIG. 7. Absorption spectrum of europium iron garnet: solid line—for $\mathbf{k} \| [100]$, $\mathbf{I} \| [001]$, $\mathbf{e} \| [010]$; dashed—for $\mathbf{k} \| [110]$, $\mathbf{I} \| [001]$, $\mathbf{e} \| [\bar{1}10]$.

$\mathbf{e} \| [001]$), we can observe the appreciable difference between them. For example, Fig. 5 has an absorption peak at a frequency $\hbar\omega = 4925$ cm^{-1}, which is not present in Fig. 1, and conversely, the peak at $\hbar\omega = 5040$ cm^{-1} is absent from Fig. 5. The two indicated curves were obtained at fixed $\mathbf{k}$ with interchange of the directions of $\mathbf{I}$ and $\mathbf{e}$, and therefore, in accordance with the existing phenomenological theories of magnetic birefringence, they should coincide. It would be natural to assume that the theory of magnetic birefringence in the region of the absorption band calls for generalization. This is the subject of the next section.

4. FEATURES OF THE PHENOMENOLOGICAL DESCRIPTION OF MAGNETIC BIREFRINGENCE IN THE REGION OF THE ABSORPTION BAND

As shown by investigations of magnetic firefringence[9] and of the orientational Faraday effect,[10] the optical and magneto-optical properties of iron garnets, which are cubic crystals, are well described far from the absorption lines by a dielectric tensor expanded up to terms not higher than the second order in the direction cosines l_i of the magnetization:

$$\hat{\varepsilon} = \varepsilon_0 + \Delta + \begin{pmatrix} \alpha l_x^2 & \beta l_x l_y + i\gamma l_z & \beta l_x l_z - i\gamma l_y \\ \beta l_x l_y - i\gamma l_z & \alpha l_y^2 & \beta l_y l_z + i\gamma l_x \\ \beta l_x l_z + i\gamma l_y & \beta l_y l_z - i\gamma l_x & \alpha l_z^2 \end{pmatrix}. \quad (1)$$

Here Δ is the contribution independent of the magnetization direction made to $\hat{\varepsilon}$ by the presence of $I(\Delta \sim I^2)$.

This form of the tensor leads to formulas for the magnetic birefringence[9] which agree naturally with the known Akulov formulas[11] for even effects in cubic crystals, for example for magnetostriction. In these formulas it is necessary only to replace the radius vector of the elongation by the unit vector $\mathbf{e}$ of the polarization of the light wave (this correspondence is valid only for normal mode).

It can be shown that regardless of the form of the employed expression for $\hat{\varepsilon}$, if the magnetization is directed along axes of the type [100] and [110], the tensor $\hat{\varepsilon}$ of cubic crystals, which is even in the magnetization, i.e., without allowance for gyrotropy, is diagonal in a coordinate system that coincides with the principal axes of the crystal. Thus, for light propagation along the [110] axis and with $\mathbf{I}$ oriented along the axes [001] and $[\bar{1}10]$, the normal modes are σ and π polarized waves. By virtue of the invariance of the Akulov formulas to interchange of the direction cosines, the expressions for the complex refractive index $\tilde{n}$ of the normal mode should coincide when the directions of $\mathbf{I}$ and $\mathbf{e}$ are interchanged, and hence also the spectra $n_{\sigma 1}(\omega)$ ($\mathbf{I} \| [001]$, $\mathbf{e} \| [\bar{1}10]$) and $n_{\sigma 2}(\omega)$ ($\mathbf{I} \| [\bar{1}10]$, $\mathbf{e} \| [001]$. From the solution of Maxwell's equations with $\hat{\varepsilon}$ in the form (1) it also follows that $n_{\sigma 1}$ and $n_{\sigma 2}$ are equal, i.e., the presence of gyrotropic terms $\sim\gamma$ in $\hat{\varepsilon}$ does not change the validity of the conclusion, with[1)] $n_{\sigma 1} = (\varepsilon_0 + \Delta - \gamma^2/\varepsilon_0)^{1/2} \approx n_{\sigma 2}$.

The symmetry of the crystal admits of a dependence of α, β, and γ on the direction cosines of the magnetization, or more accurately, on their combinations of the type $l_x^2 l_y^2 + l_y^2 l_z^2 + l_z^2 l_x^2$, $l_x^2 l_y^2 l_z^2$, etc. This dependence turns out to be significant in the region of the absorption band, when the frequency of the light is close to one of the frequencies of the transition from the ground level to an excited level of the RE ion with an environment symmetry lower than the cubic D_2, and nonequivalently arranged in the cubic lattice relative to the effective magnetic field. This fact is due to the resonant character of the dependence of α, β, and γ on the frequency of the light and the dependence of the energy of the excitation of the levels of an individual ion on the orientation of H_{eff}, i.e., the anisotropy of the G tensor of the spectroscopic splitting. The model calculation presented below is aimed qualitatively explaining the experimentally observed independence of the spectra in $\mathbf{I}$ and $\mathbf{e}$, and also point the way towards constructing a generalized phenomenological theory of magnetic birefringence. Instead of the experimentally investigated transitions $^7F_0 \to {}^7F_6$ we consider a simpler transition of the type $J=0 \to J=1$. The calculation is illustrative in character and does not take into account all the features of the interaction of the magnetic ions in a real iron garnet crystal, for example the shifts of the wave functions of the RE ions in different nonequivalent points, interaction between the iron and RE sublattices, anisotropic exchange, noncubic distortions of the lattice, and others.

We consider the transition from the ground level $J=0$ to the triplet level $J=1$ of the RE ion with account taken of the six equivalent points that it can occupy in the cubic lattice, and we establish the form of the tensor $\hat{\varepsilon}$ within the framework of the chosen model. To take into account the local symmetry of the environment, we shall assume the G tensor to be anisotropic with principal values G_x, G_y, G_z, and assume that the crystal field is directed along the z axis of the local coordinate system in which the G tensor is diagonal.

Starting from the model Hamiltonian[12]

$$\mathcal{H} = \mathcal{H}_0 + G_x J_x H_x + G_y J_y H_y + G_z J_z H_z + D[3J_z^2 - J(J+1)],$$

where $J = L + S$ and D characterizes the splitting of the levels J at $H_{eff} = 0$, we obtain for the components of the tensor $\tilde{\varepsilon}_{ij}$ of a single ion, expressed in the local coordinate system, the following equation (we neglect the difference between the populations of the levels split by H_{eff} and D)

$$\tilde{\varepsilon}_{ij} = \varepsilon_{ij}^0 + \zeta \sum_{k=1}^{3} \frac{F_{ij}^{(k)}}{E - E_k + i\Gamma_k - E_0} + \frac{F_{ji}^{*(k)}}{E + E_k + i\Gamma_k + E_0},$$

$$F_{xx}^{(k)} = \frac{(D-E_k)^2 G_y^2 l_y^2 + G_z^2 G_x^2 l_x^2 l_z^2}{Q_k}, \quad F_{yy}^{(k)} = \frac{(D-E_k)^2 G_x^2 l_x^2 + G_z^2 G_y^2 l_z^2 l_y^2}{Q_k},$$

$$F_{zz}^{(k)} = \frac{[(D-E_k)^2 - G_z^2 l_z^2]^2}{Q_k}, \quad F_{ij\,(i \neq j)}^{(k)} = \frac{[(D-E_k)^2 - G_z^2 l_z^2] G_i G_j l_i l_j}{Q_k}, \quad (2)$$

$$Q_k = (G_x^2 l_x^2 + G_y^2 l_y^2)[G_z^2 l_z^2 + (D-E_k)^2] + [(D-E_k)^2 - G_z^2 l_z^2]^2,$$

where ε_{ij}^0 takes into account other optical transitions, for example of the charge-transfer type, l_i are the direction cosines of the magnetization, ζ is a certain small parameter ($\zeta \ll 1$) and characterizes the magnitude of the magnetic linear birefringence and dichroism, E is the photon energy, E_0 is the energy of the center of gravity of the level $J=1$ split into sublevels (this energy is reckoned from the ground level), $E_k + E_0$ is the energy of the split levels

$$E_1 = 2v^{1/2} \cos(^1/_3 \arccos r), \quad E_{2,3} = -2v^{1/2} \cos(^1/_3 \arccos r \pm \pi/3)$$

$$r = -\frac{2D^3 + D(G_x^2 l_x^2 + G_y^2 l_y^2 - 2G_z^2 l_z^2)}{2v^{3/2}}, \quad v = D^2 + {}^1/_3 (G_z^2 l_z^2 + G_y^2 l_y^2 + G_x^2 l_x^2),$$

and we always have $|r| \leq 1$. Averaging over all 6 positions of the RE ion, we obtain for the dielectric tensor of the crystal as a whole the expression

$$\hat{\varepsilon} = \frac{1}{6}\sum_{p=1}^{6} T_p^{-1}\hat{\varepsilon}(T_p I)T_p = \frac{1}{6}\sum \hat{\varepsilon}_p', \tag{3}$$

where T_p are unitary matrices of the rotation from the tetragonal axis of the crystal to the local axis of the p-th position ($p = 1-6$).

The tensor $\hat{\varepsilon}$ is compatible with the symmetry group of the cubic crystal. At $G_x = G_y = G_z$ and $D = 0$ we obtain the tensor $\hat{\varepsilon}(1)$ with $\alpha = \beta$, corresponding to a uniaxial crystal. Figure 8 shows the calculated absorption spectra of σ polarized waves for two magnetization directions, $\mathbf{I} \| [001]$ and $\mathbf{I} \| [\bar{1}10]$. It is seen that the spectra do not coincide in the region of the absorption band, and approach each other asymptotically far from the absorption lines of the RE ions. The appearance of a small peak C between the principal intensive lines A and B, a peak seen even on the experimental curves, is due to the G-tensor anisotropy that leads to a partial shift of the σ and π spectra corresponding to the isotropic G tensor. The difference between the intensities of the components A and B is due to the shift of the functions because of the action of the crystal field. At $D = 0$ the spectra are symmetrical. Thus, the considered rough model explains qualitatively some features of the experimental spectra reported in Sec. 3 of the present paper. Figure 9 shows the calculated plots of the quantity

$$\eta(\tau) = \left| \frac{\mathrm{Im}(\varepsilon_{\sigma 1} - \varepsilon_{\sigma 2})}{\mathrm{Im}(\varepsilon_{\sigma 1} + \varepsilon_{\sigma 2})} \right|$$

of the relative change of $\mathrm{Im}\,\varepsilon_0$ with changing orientation of the field from $\mathbf{I} \| [001]$ to $\mathbf{I} \| [\bar{1}10]$ for two values of the photon energy in relative units, $E = 10$ and $E = 30$ (only terms even in I are taken into account in $\hat{\varepsilon}$). The quantity τ characterizes the difference between G_x and G_y: $G_x = G_z(1+\tau)$, $G_y = G_z(1-\tau)$. Far from the absorption band ($E = 30$) the $\mathrm{Im}\,\varepsilon_\sigma \sim k$ spectra almost coincide ($\eta \sim 1\%$), whereas near the absorption lines $\eta \sim 15\%$ ($\tau = 0.5$). The main cause of the difference between $\mathrm{Im}\,\varepsilon_{\sigma 1}$ and $\mathrm{Im}\,\varepsilon_{\sigma 2}$ is the dependence of the energies of the excited levels on the orientation of I, and consequently on the maxima on the absorption curve. Far from the absorption lines this difference turns out to be inessential, since the position of the "center of gravity" of the split levels does not depend on the orientation of the I.

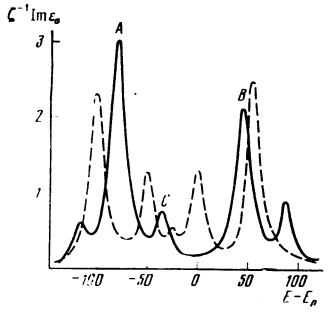

FIG. 8. Calculated spectra of $\zeta^{-1}\,\mathrm{Im}\,\varepsilon_\sigma$, illustrating the independence of the σ spectra to the interchange of I and e ($\Gamma_x = 3$, $G_x = 20$, $G_y = 40$, $G_z = 10$, $D = 10$); solid line—for $\mathbf{I} \| [\bar{1}10]$, $\mathbf{e} \| [001]$; dashed—for $\mathbf{I} \| [001]$, $\mathbf{e} \| [\bar{1}10]$.

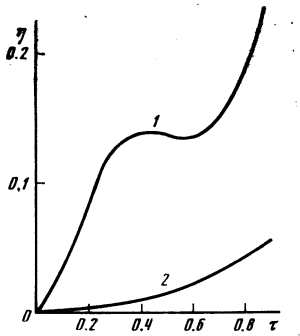

FIG. 9. Dependence of the relative difference of Im ε_σ at $\mathbf{I} \| [\bar{1}10]$, $\mathbf{e} \| [001]$ and $\mathbf{I} \| [001]$, $\mathbf{e} \| [\bar{1}10]$ on the G-tensor anisotropy τ at fixed $G_z = 10$; curve 1—$E = 10$, 2—$E = 30$.

An analysis of formula (2) and (3) shows that in the resonance region, when the frequency of the light is close to one of the frequencies of the transition of the RE ion from the ground state to an excited state, it becomes essential to take into account in $\hat{\varepsilon}$ orders of l_i higher than the second. This is due to the presence of nonequivalent points in the RE sublattice of the iron garnet. It follows therefore that the motion of the optical axis with changing direction of I is not described by the formulas obtained in Ref. 13. Far from the absorption lines ($E \gg E_0$) the tensor $\hat{\varepsilon}$ given by Eqs. (2) and (3) goes over asymptotically into (1). It can be assumed that the anisotropy of the exchange interaction leads to analogous qualitative consequences relative to the behavior of the magnetic birefringence in the region of the absorption band.

[1)]Calculation yields $n_{\sigma 2}^2 = \varepsilon_0 + \Delta - 4\gamma^2/(4\varepsilon_0 + 4\Delta + \alpha - \beta) \approx \varepsilon_0 + \Delta - \gamma^2/\varepsilon_0 - (\gamma^2\Delta/\varepsilon_0^2 + \gamma^2(\alpha - \beta)/\varepsilon_0^2 + \ldots)$. Since the contribution to $n_{\sigma 2}$, which is proportional to I^4, I^6, etc. is due not only to the terms in the brackets, but also to the next higher terms of the expansion of ε in I, which are not taken into account in (1), a correct approximation is $n_{\sigma 2}^2 \approx \varepsilon_0 + \Delta - \gamma^2/\varepsilon_0$.

[1]J. F. Dillon, Jr., J. Appl. Phys. **29**, 1286 (1958).
[2]G. S. Krinchik and G. K. Tyutneva, Zh. Eksp. Teor. Fiz. **46**, 435 (1964) [Sov. Phys. JETP **19**, 292 (1964)].
[3]R. V. Pisarev, I. G. Siniĭ, and G. A. Smolenskiĭ, Zh. Eksp. Teor. Fiz. **57**, 737 (1969) [Sov. Phys. JETP **30**, 404 (1969)]. J. F. Dillon, Jr., J. P. Remeika, and C. R. Staton, J. Appl. Phys. **41**, 4613 (1970). R. V. Pisarev, I. G. Silin, N. N. Kolpakova, and Yu. M. Yakovlev, Zh. Eksp. Teor. Fiz. **60**, 2188 (1971) [Sov. Phys. JETP **33**, 1175 (1971)].
[4]P. M. Levy, Phys. Rev. **A135**, 155 (1964). R. L. Green, D. D. Sell, W. H. Yen, A. L. Schawlow, and K. M. White, Phys. Rev. Lett. **15**, 656 (1965). T. Moriya, J. Appl. Phys. **39**, 1042 (1968). G. S. Krinchik and M. V. Chetkin, Usp. Fiz. Nauk **98**, 3 (1969) [Sov. Phys. Usp. **12**, 307 (1969)]. V. V. Eremenko and A. I. Belyaeva, Usp. Fiz. Nauk **98**, 27 (1969) [Sov. Phys. Usp. **12**, 320 (1969)].
[5]K. A. Wickersheim, Phys. Rev. **122**, 1376 (1961).
[6]E. Orlich, S. Hüfner, and P. Grünberg, Z. Phys. **231**, 144 (1970). D. Boal, P. Grünberg, and J. A. Koningstein, Phys. Rev. **B7**, 4757 (1974). V. Nekvasil, V. Roskovec, and F. Lounová, J. Appl. Phys. **49**, 1471 (1978). I. A. Koningstein, Usp. Khim. **42**, 1810 (1973).
[7]G. S. Krinchik, Fiz. Tverd. Tela (Leningrad) **5**, 373 (1963). [Sov. Phys. Solid State **5**, 273 (1963)].
[8]G. S. Krinchik and M. V. Chetkin, Zh. Eksp. Teor. Fiz. **41**,

673 (1961) [Sov. Phys. JETP 14, 485 (1961)].
[9]G. A. Smolenskiĭ, R. V. Pisarev, and I. G. Sinif, Usp. Fiz. Nauk 116, 231 (1975) [Sov. Phys. Usp. 18, 410 (1975)].
[10]I. G. Avaeva, F. V. Lisovskiĭ, and V. I. Shapovalov, Mikroélektronika (Akad. Nauk SSSR) 2, 337 (1973).
[11]N. S. Akulov, Ferromagnetizm (Ferromagnetism), Gostekhizdat, 1939.
[12]A. Abragam and B. Bleaney, Electron Paramagnetic Resonance, Oxford, 1970.
[13]R. V. Pisarev, Fiz. Tverd. Tela (Leningrad) 17, 1396 (1975) [Sov. Phys. Solid State 17, 898 (1975)].

Translated by J. G. Adashko